JOURNAL OF MATERIALS SCIENCE 29 (1994) 1873–1878

Synthesis and crystallization of yttrium–aluminium garnet and related compounds

N. J. HESS, G. D. MAUPIN, L. A. CHICK, D. S. SUNBERG, D. E. McCREEDY, T. R. ARMSTRONG
Pacific Northwest Laboratory, Richland, Washington 99352, USA

Amorphous oxide combustion products with compositions corresponding to $Y_4Al_2O_9$, $YAlO_3$, and $Y_3Al_5O_{12}$ were synthesized by the glycine–nitrate process and heat-treated to induce crystallization. The crystalline structure of the resulting powders was determined by powder X-ray diffraction techniques. The phase stabilities of the crystalline phases were investigated as functions of the glycine-to-nitrate ratio, the yttrium-to-aluminium ratio, and the heat-treatment conditions. Heat treatment for short durations resulted in incompletely crystalline powders that consisted of a mixture of $Y_4Al_2O_9$, $YAlO_3$, and $Y_3Al_5O_{12}$ phases, regardless of the chemical composition of the amorphous combustion product. However, heat treatment for longer durations or higher temperature generated both pure-phase, monoclinic $Y_4Al_2O_9$ and $Y_3Al_5O_{12}$ with the garnet structure. Prolonged heat treatment at high temperature failed to generate pure-phase orthorhombic $YAlO_3$. Subsequent analysis revealed a sluggish, complex crystallization process involving the formation and decomposition of several phases.

1. Introduction

Interest in the Y_2O_3–Al_2O_3 system stems from high-temperature ceramic applications and, over the past 20 years, has grown because cubic $Y_3Al_5O_{12}$ (YAG) is important in solid-state laser applications [1]. Recently, a novel pressure-temperature monitoring technique, based on the fluorescence of samarium-doped YAG, has been developed [2]. The work presented here is in support of this sensor development project and is directed toward production of phase-pure, polycrystalline YAG doped with a variety of rare-earth cations. Knowledge of the crystallization process gained from this study is now being applied to production of YAG thin films [3].

Three intermediate compounds, $Y_3Al_5O_{12}$, $YAlO_3$, and $Y_4Al_2O_9$ exist within the Y_2O_3–Al_2O_3 system [4]. Crystalline $Y_3Al_5O_{12}$ normally exists in a cubic form with the garnet structure and is commonly known as "yttrium aluminium garnet" or YAG [5]. A high-temperature tetragonal polymorph has also been reported [6]. Crystalline $YAlO_3$, "yttrium aluminum perovskite" or YAP, has orthorhombic [7] and hexagonal [8] polymorphs. Crystalline $Y_4Al_2O_9$ is monoclinic and is referred to as YAM [9]. These terms have been used to signify both composition and structure of the compound; however some confusion arises when these terms are used to refer to the chemical composition of the precursor. In this paper the terms YAG, YAP and YAM will be used to refer to the crystalline compounds, but the formulaic representation, i.e. $Y_3Al_5O_{12}$, $YAlO_3$ and $Y_4Al_2O_9$, will be used when discussing the chemical composition of the precursor material or combustion product. The following paragraph briefly reviews the variety of synthesis techniques that have been employed to synthesize these materials and knowledge of phase stability within the Y_2O_3–Al_2O_3 system.

Before 1974, the phase diagram of the Y_2O_3–Al_2O_3 system was based mainly on high-temperature sintering of mechanical mixtures of the oxide starting material, and is summarized by Abell *et al.* [10]. Briefly, YAP was reported to have a limited range of stability, between 1835 °C and 1875 °C [11], and to be unstable below 1600 °C [12]. The YAP and YAM phases were observed to decompose to YAG, and unknown "X" composition at elevated temperatures [10]. Based on their own results, Abell *et al.* concluded that YAG was the only stable compound within the system, and that YAP and YAM were both metastable compounds [10]. Other researchers have reported YAP to be, "a first product" [9, 13], "one of several first products" [14, 15], or "an intermediate product" [6, 16, 17].

The Czochralski technique has been used to pull large, single-crystal yttro-aluminates from melts. Single-crystal growth studies have indicated the stability range for YAG to be from room temperature to 1970 °C; for YAP, from room temperature to 1870 °C; and for YAM from 1000 °C to 1930 °C [1]. Other synthesis methods include solid-state reactions which use repetitive alternation of heating and grinding [13, 16, 18]; hydrolysis of metal-alkoxides [19]; hydroxide co-precipitation [20], and polyesterized malonic acid/metal-nitrate thermal decomposition [21]. The

0022–2461

crystallization of YAG from an amorphous starting material was reported by Yamaguchi *et al.* [19] and Veitch [21] to involve a two-step transformation involving either a hexagonal YAP–Al_2O_3 solid solution [19] or a YAP–amorphous alumina mixture [21] intermediate. YAG has also been synthesized by urea–carbohydrazide combustion processes [22]. In this technique, metal nitrates (oxidizers) and a urea–carbohydrazide (fuel) are dissolved in water and then rapidly heated in a muffle furnace. The precursor solutions spontaneously ignite and burn, resulting in a voluminous, crystalline, single-phase product. In the present study, YAG, YAP and YAM are produced by heat-treating powders synthesized by a combustion technique similar to the urea–carbohydrazide process. In this study, however, glycine was used as a fuel and the combustion product is X-ray amorphous.

2. Experimental procedure

The glycine-nitrate process is a self-sustaining combustion synthesis technique that produces fine, homogeneous metal-oxide powders. Aqueous precursor solutions containing metal nitrates and glycine are heated on a hot plate until they auto-ignite, producing metal-oxide "ash". Glycine serves a dual role in the glycine-nitrate process. In the precursor solution, the glycine complexes the metal cations, thereby preventing selective precipitation. Upon ignition, the glycine is oxidized by the nitrate anions, thereby serving as the fuel for the combustion reaction [23].

In this study, both the aluminium-to-yttrium cation ratio and the glycine-to-nitrate (fuel-to-oxidant) ratio were systematically varied in the precursor solutions. Metal nitrate stock solutions were made from reagent grade chemicals and deionized water ($\sim 10^{18}$ megohms cm^{-1}). Stock solution molalities were then determined using ethylene diaminetetreacetic acid (EDTA) titration techniques [24]. Appropriate amounts of aluminium and yttrium solutions, corresponding to the desired molar cation ratios, were weighed out and combined with various amounts of glycine. A "stoichiometric" glycine-to-nitrate ratio was calculated by assuming complete combustion; in other words, the required amount of glycine was determined by assuming that the sole gaseous products of combustion were H_2O, CO_2 and N_2, with all nitrates and glycine consumed and with no atmospheric oxygen required [25]. 'Fuel-lean' and 'fuel-rich' conditions were calculated by dividing the stoichiometric glycine quantity in half or doubling the glycine quantity, respectively.

Combustion of the precursor solutions were performed batch-wise in a 500-ml Pyrex beaker using 10–20 ml precursor solution per burn. The glycine-nitrate process applied to the Y_2O_3–Al_2O_3 system produced relatively slow reactions which lasted several seconds. In contrast, glycine-nitrate synthesis of chromites under similar conditions produces rapid, vigorous reactions lasting about 1 s [23, 25].

The combustion products were heat-treated by placing about 2 g of sample into high-purity alumina boats. The boats were then loaded into an electric resistance-heated muffle furnace in air. Heat treatment followed one of two protocols. The majority of the samples were heat-treated following protocol A: the boats were placed on cold furnace, heated at a rate of 300 °C per hour, soaked at a prescribed temperature for a given duration, and cooled to room temperature at 300 °C h^{-1}. For $Y_3Al_5O_{12}$ and $YAlO_3$ compositions, which were known to exhibit a complex crystallization sequence, the samples were heat-treated following protocol B: the boats were placed in a preheated furnace for a given period of time and quenched to room temperature.

The crystallinity of the samples was determined using X-ray diffraction analysis (XRD). A Phillips, APD 3620 powder diffractometer, graphite monochromator, and copper target X-ray tube were used. Diffraction patterns were recorded in step-scan mode (0.02 °2θ intervals, 1 s sampling time) over a range of 10 to 70 ° 2θ. All data were collected at room temperature. Lattice parameters for selected samples were determined with the aid of an internal silicon standard and refined using a linear least-squares regression technique. For these samples, diffraction patterns were recorded over a range from 10 to 125 ° 2θ, at 0.02 ° 2θ step intervals, and for a 10-s sampling time.

3. Results and discussion

3.1. Glycine-to-nitrate ratio

For all sample compositions, the glycine-nitrate combustion product, (ash) yielded very broad XRD peaks, similar to the pattern shown in Fig. 1. This particular sample has $Y_3Al_5O_{12}$ composition and was prepared under fuel-lean combustion conditions. Samples combusted under stoichiometric or fuel-rich combustion conditions generated XRD patterns essentially identical to Fig. 1. These broad patterns are indicative of amorphous material or of microcrystalline material.

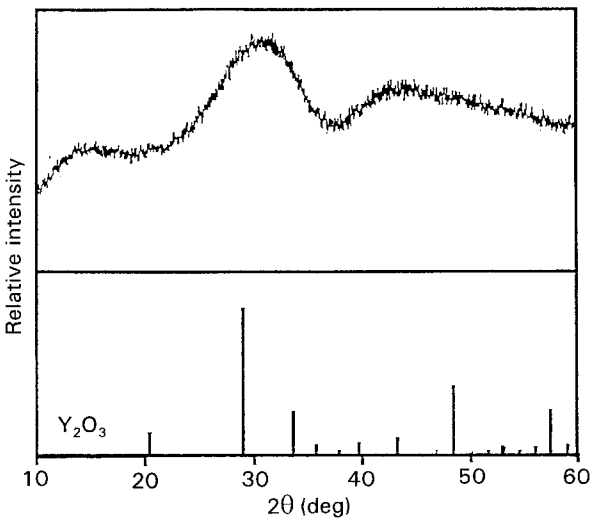

Figure 1 Top is an XRD pattern from a combustion product having $Y_3Al_5O_{12}$ stoichiometry, produced under fuel-lean conditions via the glycine-nitrate synthesis technique. Although the material is X-ray amorphous, the positions of the extremely broad peaks suggest that microcrystalline Y_2O_3 may be present.

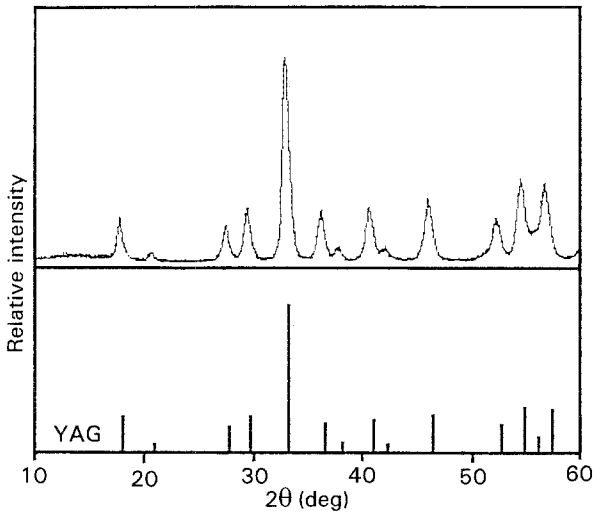

Figure 2 Diffraction pattern of the material shown in Fig. 1 following heat treatment at 1000 °C for 30 min by protocol A. The pattern is indicative of material composed of ~ 20-nm crystallites of phase-pure YAG with little amorphous material remaining.

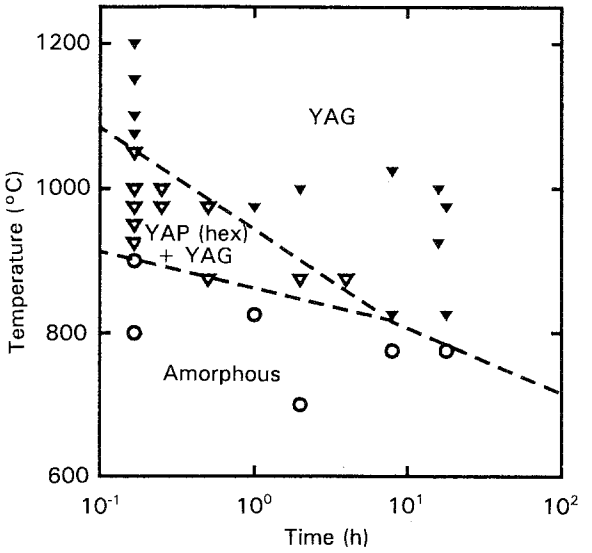

Figure 3 Time–temperature plot showing crystalline phases for starting materials with $Y_3Al_5O_{12}$ composition. Samples plotted were prepared following protocol A or B. Broken lines are boundaries indicating approximate minimum time or temperature required to cause a given transformation. ○ X-ray amorphous ash; △, presence of hexagonal YAP and YAG; ▼, presence of pure-phase YAG.

Fig. 2 shows the XRD pattern for the same material as in Fig. 1, but after heat treatment at 1000 °C for 30 min by protocol A. The diffraction peaks in Fig. 2 are relatively broad, indicative of material composed of approximately 20-nm crystallites of phase-pure YAG with little amorphous material remaining. The same heat treatment performed on material combusted under stoichiometric and fuel-rich conditions produced samples containing minor amounts of hexagonal YAP along with YAG, indicating that fuel-lean combustion favoured subsequent YAG crystallization. All subsequent samples were prepared under fuel-lean combustion conditions.

3.2. Multi-step crystallization processes

Crystallization combustion products with $YAlO_3$ and $Y_3Al_5O_{12}$ composition were observed to follow multi-step transformations to the fully crystalline state. Crystallization of YAG from an ash with $Y_3Al_5O_{12}$ composition appears to involve the formation of the hexagonal YAP as an intermediate as shown in the temperature–time diagram in Fig. 3. At a temperature 800 °C for 8 h, YAG appears to crystallize directly from the amorphous ash. However, at higher temperature and shorter duration, hexagonal YAP is observed to form as a metastable intermediate, as shown in Fig. 4. Fig. 4a shows the 25–35° 2θ portion of an XRD sample pattern with the reference patterns for hexagonal YAP (JCPDS # 16-219) and YAG (JCPDS # 33-40). Both of these phases are present in the particular sample pattern shown. Fig. 4b illustrates the isothermal crystallization of ash having $Y_3Al_5O_{12}$ composition at 925 °C. After 15 min, the powder consisted of approximately equal proportions of hexagonal YAP and YAG. After 30 min, YAG was more prevalent than hexagonal YAP and the overall intensity of the pattern increased. After 16 h, only phase-pure YAG was apparent.

These results suggest that YAG can crystallize by one of two pathways: first, directly from an amorph-

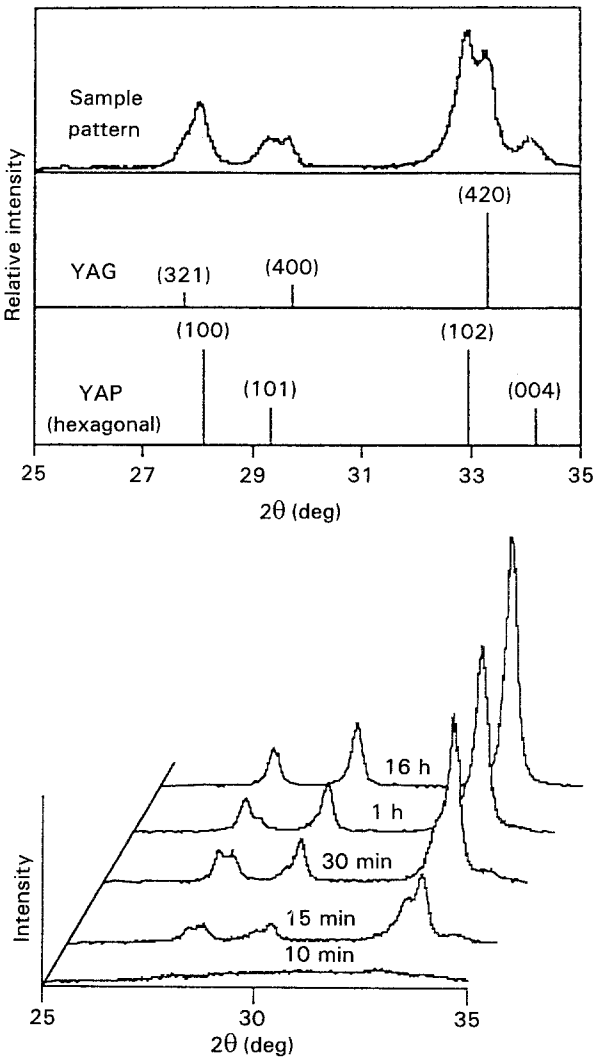

Figure 4 Portions of XRD patterns from 25 to 35° 2θ, for samples with YAG stoichiometry, heat-treated at 925 °C following protocol B for a range of times. Hexagonal YAP is detectable at the intermediate times.

ous ash with the same composition, and second (as illustrated in Fig. 4b) from the transformation of hexagonal YAP. The second pathway raises two related issues: If YAG and YAP are stoichiometric phases, what happens to the excess Al when YAP is present, and by what process does the transformation from YAP to YAG occur? The YAP to YAG transformation requires either: (i) solid-state reaction, the diffusion of Al into hexagonal YAP crystallites followed a structural transformation to the garnet structure; (ii) transformation, the nucleation and growth of hexagonal YAP with $Y_3Al_5O_{12}$ stoichiometry followed by transformation to the garnet structure; or (iii) decomposition, the reabsorption or disassociation of hexagonal YAP to the amorphous state prior to the continued crystallization of YAG.

Recent work by Yamaguchi *et al.* [26] addresses these issues. Briefly, these authors prepared amorphous Y_2O_3–Al_2O_3 material from alkoxides with varied Al content, and crystallized the amorphous material at a rate of 600 °C h^{-1}. After temperatures between 970 and 1050 °C had been attained, the *c* lattice parameter (determined using powder XRD techniques) of the hexagonal YAP phase was found to decrease with the increasing Al content of the starting material. From these results, and from DTA analysis, Yamaguchi *et al.* concluded that the excess Al resulting from the crystallization of YAP was accommodated by the substitution of Al for Y in hexagonal YAP itself. This conclusion contrasts with the earlier work of Veitch [21] who prepared $Y_3Al_5O_{12}$ precursor from a solution of metal nitrates, glycerol and malonic acid. On the basis of the lack of XRD peaks corresponding to crystalline Al_2O_3 and the rapidity of the conversion of YAP to YAG, Veitch suggests that the excess Al exists as amorphous Al_2O_3.

In an effort to resolve this discrepancy, lattice parameters were determined for the YAP and YAG phases in two samples, one sample with $Y_3Al_5O_{12}$ composition that had been heat-treated for 10 min at 1000 °C, and the second sample with $YAlO_3$ composition that had been heat-treated at 875 °C for 24 h. Both samples were highly crystalline, and YAG and YAP each constituted at least 25 wt % of the sample. The *c* and *a* lattice parameters of YAP and the *a* lattice parameter of YAG did not significantly differ between the two samples. These results imply that excess Al is not accommodated by the substitution of Al for Y in YAP, and that excess Al probably resides in a separate, amorphous phase, as concluded by Veitch [21].

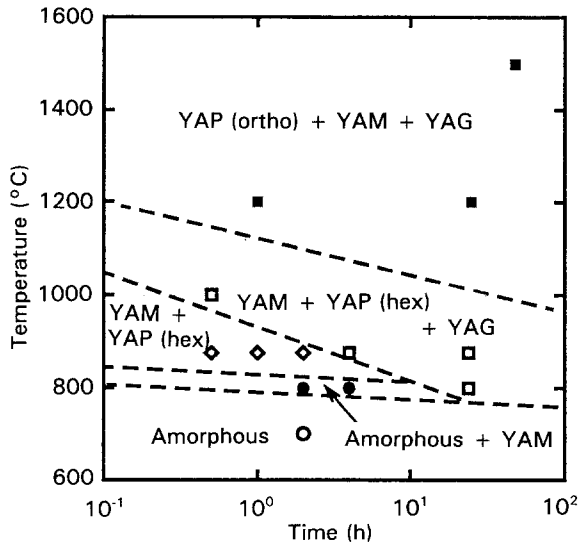

Figure 5 Time–temperature plot similar to Fig. 3, but for starting materials having $YAlO_3$ composition. ○, amorphous ash; ●, presence of YAM; ◇, presence of YAM and hexagonal YAP; □, assemblage of YAM, hexagonal YAP and YAG; ■, assemblage of orthorhombic YAP, YAM and YAG.

Crystallization of orthorhombic YAP from a composition product with $YAlO_3$ composition is more complex, involving three intermediate phases: hexagonal YAP; YAM; and YAG, as shown in the temperature–time diagram in Fig. 5. At the highest temperature and longest duration, 1500 °C and 24 h, the sample consisted of predominately orthorhombic YAP with only a trace of YAG and YAM. Although the crystallization process is complex, the observations summarized in Fig. 5 suggest that crystallization of ash with $YAlO_3$ composition can be represented by the following highly idealized reaction:

Amorphous $YAlO_3$ → YAM →

hexagonal YAP → YAG → orthorhombic YAP

As discussed above, the transformation from one crystalline phase to another can follow a number of pathways. This reaction pathway differs significantly in the sequence of observed phases from the reaction process reported by Yamaguchi [26]. These differences may result from the choice of starting materials and heat treatment protocols.

Although the synthesis of YAM was not a focus of this study, limited results suggest that crystallization of $Y_4Al_2O_9$ ash to YAM also follows a multi-step transformation. Heat treatment at 1200 ° for 1 h resulted in the formation of an orthorhombic YAP and YAM. Extended heat treatment at 1500 °C resulted in pure-phase YAM. On the basis of the crystallization of $YAlO_3$ and $Y_3Al_5O_{12}$ ash, it is likely that heat treatment at lower temperatures would result in an assemblage consisting of YAM and hexagonal YAP. The crystallization sequence can be represented as:

Amorphous $Y_4Al_2O_9$ → hexagonal YAP →

orthorhombic YAP → YAM

3.3. Yttrium-to-aluminium ratio

In order to investigate the stability of YAM, YAP and YAG as a function of composition, a series of combustion products were prepared with varied Al_2O_3-to-Y_2O_3 ratios. Ten different compositions, from to 85 mol % Al_2O_3 (Al-rich relative to YAG, $Y_3Al_5O_{12}$) to 16.7 mol % Al_2O_3 (Y-rich relative to YAM, $Y_4Al_2O_9$), were prepared and heat-treated at 1200 °C for 1 h, following protocol A. The approximate weight fraction of the resulting crystalline phases, as determined by the relative XRD peak intensities, is

represented in Fig. 6. Note, however, that amorphous material is not represented here and may constitute a portion of some samples. The results for samples with $Y_3Al_5O_{12}$ and $YAlO_3$ compositions have been discussed in the above section; results for samples that are 'off-stoichiometry' are presented below.

As shown in Fig. 6, heat treatment of materials with compositions only slightly depleted in Al content, relative to YAG stoichiometry, resulted in the formation of powders that consisted of YAG with a minor, but detectable, amount of YAM. However, samples that were crystallized with excess Al relative to YAG stoichiometry did not form a second crystalline phase, Al_2O_3, until the Al was moderately enriched, at 70.3 mol% Al_2O_3. For the composition with 67.7 mol% Al_2O_3 the crystallized powder contained YAG as the only detectable crystalline phase. Thus, it can be interpreted that the garnet structure excludes significant levels of Y substitution for Al, while accommodating significant Al substitution for Y. Alternatively, the excess Al in this sample may have been present as X-ray amorphous Al_2O_3. This alternative seems more plausible, based on crystal chemistry considerations: in the garnet structure, Y occupies a site that is coordinated by eight oxygens and, as a result can accommodate large cations. Al occupies two distinct sites, coordinated by six and four oxygens, that can only accommodate smaller cations. Substitution of Y into the six-coordinate Al site would result in the distortion of the oxygen octahedron, necessitating an increase in oxygen–oxygen bond lengths. Such an increase in bond lengths is energetically unfavourable because the octahedron shares six oxygen–oxygen edges with other polyhedra, thereby transmitting large lattice strain. Thus it is not surprising that the samples on the Y-enriched side of YAG produced a second crystalline phase to accommodate the excess Y. On the other hand, an Al cation substituted into the eight-coordinate Y site in YAG would 'rattle' inside the oxygen dodecahedron because the ionic radius of Al is approximately half that of Y [27]. This situation is also energetically unfavourable, because the Al would not be in close contact with the surrounding oxygen anions [28].

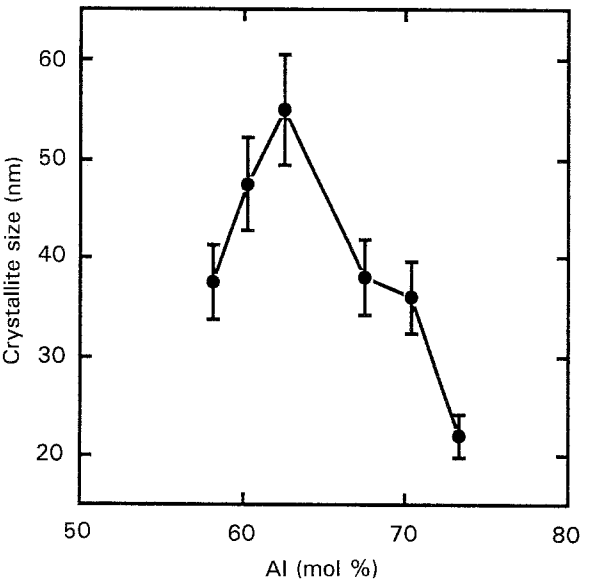

Figure 7 Crystallite size of the YAG phase detected in samples with compositions at or near stoichiometric YAG. The largest YAG crystals are formed in the sample having YAG stoichiometry.

Variation of the yttrium-to-aluminium ratio of the combustion product also affected the crystallite size of YAG that grew during heat treatment, as shown in Fig. 7. These data, determined by measurement of XRD peak widths for samples heated by protocol A to 1200 °C for 1 h, indicate that maximum crystallite size was attained for ash with stoichiometric YAG composition. The interpretation of grain growth in the solid state involves many issues, such as the diffusion rates of the diffusing species, the competition for cations by co-existing phases, and the free energy of crystallization the crystallizing phase [29–31]. However the results of these experiments, in which the composition of the system affects the resulting crystallite size, suggest that both the rate of diffusion and the free energy of crystallization are dominant controls on grain growth.

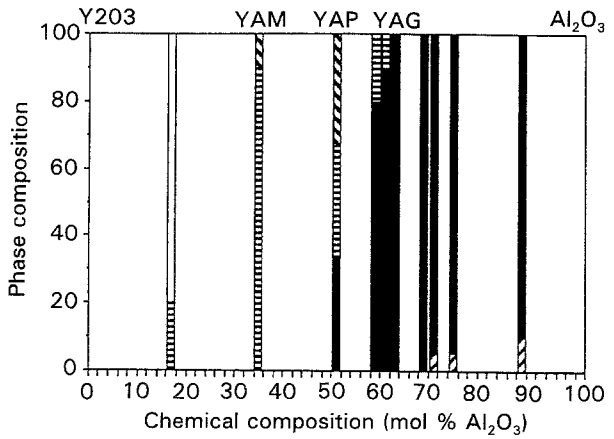

Figure 6 Approximate weight fraction of crystalline products resulting from 1200 °C, 1-h heat treatment using protocol A of materials with varying yttria-to-alumina ratios. ▨ Al_2O_3; ■, YAG; ▤ YAM; ▧ YAP (ortho); □, Y_2O_3.

4. Conclusions

Discrepancies within the literature concerning the stabilities and formation of the intermediate compounds in the Al_2O_3–Y_2O_3 system are probably due to the complex reaction pathways and kinetics. In this work highly crystalline, phase-pure YAM and YAG powders were synthesized. However, neither phase-pure hexagonal YAP or orthorhombic YAP could be generated. It is suggested that crystallization of amorphous material with YAP stoichiometry follows the sequence: amorphous → YAM → hexagonal YAP → YAG → orthorhombic YAP. The formation of YAG can follow two routes: below about 825 °C, YAG appears to form directly from the amorphous material, while at higher temperatures, hexagonal YAP appears to form as a metastable phase. Results of the current study indicate that neither YAP nor YAG deviate appreciably from stoichiometry.

Acknowledgements

D. S. S was supported by the Northwest College and University Association for Science (Washington State University) under Grant DE-FG06-89ER-75522 with the US Department of Energy. Pacific Northwest Laboratory is operated by Battelle Memorial Institute for the US Department of Energy under contract DE-AC06-76RLO 1830.

References

1. B. COCKAYNE, *J. Less-Common Metals* **114** (1985) 119.
2. N. J. HESS and D. SCHIFERL, *J. Appl. Phys.* **71** (1992) 2082.
3. N. J. HESS, G. J. EXARHOS and S. M. WOOD, *Mater. Res. Soc. Symp. Proc.* **244** (1992) 281.
4. A. F. WELLS, in "Structural inorganic chemistry", (Clarendon Press, Oxford, 1975) p. 1095
5. H. S. YODER and M. L. KEITH, *Amer. Mineral.* **36** (1951) 519.
6. M. L. KEITH and R. ROY, *ibid.* **39** (1954) 1.
7. S. GELLER and E. A. WOOD, *Acta Crystallogr.* **9** (1956) 536.
8. F. BERTAUT and J. MARESCHAL, *C. R. Hebd. Seances Acd. Sci.* **257** (1963) 867.
9. I. WARSHAW and R. ROY, *J. Amer. Ceram. Soc.* **42** (1959) 434.
10. J. S. ABELL, I. R. HARRIS, B. COCKAYNE and B. LENT, *J. Mater. Sci.* **9** (1974) 527.
11. N. A. TOROPOV, I. A. BODNAR, F. YA GALADHOV, Kh. S. NIKOGOSYAN and N. V. VINOGRADOVA, *Izv. Akad. Nauk SSSR, Ser. Khim.* **7** (1969) 1158.
12. M. MIZUNO and T. NOGUCHI, *Rep. Gov. Ind. Res. Inst. Nagoya* **16** (1967) 171.
13. R. S. ROTH, *J. Res. N.B.S.* **58** (1957) 75.
14. S. NAKA, O. TAKENAKA, T. SEKIYA and T. NODA, *Kogyo Kagaku Zasshi* **69** (1966) 1112.
15. T. NOGUCHI and M. MIZUNO, *Rep. Gov. Ind. Res. Inst. Nagoya* **70** (1967) 834.
16. S. J. SCHNEIDER, R. S. ROTH and S. J. WARING, *J. Res. N.B.S.* **65A** (1961) 345.
17. V. B. GLUSHOKOVA and L. P. KACHALOVA, *Izv. Akad. Nauk SSSR, Neorg, Mater.* **19** (1983) 95.
18. W. CLASS, *J. Crystal Growth* **3, 4** (1963) 241.
19. O. YAMAGUCHI, K. TAKEOKA and A. HAYASHIDA, *J. Mater. Sci. Lett.* **10** (1990) 101.
20. H. HANEDA, in "Metal, inorganic and polymer materials" (Japan Foundation of Scientific Technology Information, Tokyo, 1987) p. 720.
21. C. D. VEITCH, *J. Mater. Sci.* **26** (1991) 6527.
22. J. J. KINGSLEY, K. SURESH and K. C. PATIL, *J. Solid State Chem.* **87** (1990) 435.
23. L. A. CHICK, L. R. PEDERSON, G. D. MAUPIN, J. L. BATES, L. E. THOMAS and G. J. EXARHOS, *Mater. Lett.* **10** (1990) 6.
24. C. N. REILLEY and R. W. SCHMIDT, *Anal. Chem.* **30** (1958) 947.
25. L. A. CHICK, G. D. MAUPIN, G. L. GRAFF, L. R. PEDERSON, D. E. MCCREADY and J. L. BATES, *Mater. Res. Soc. Symp.* **249** (1992) 159.
26. O. YAMAGUCHI, K. TAKEOKA, K. HIROTA, H. TAKANO and A. HAYASHIDA, *J. Mater. Sci.* **27** (1992) 1261.
27. R. D. SHANNON, *Acta Cryst.* **A32** (1976) 751.
28. L. PAULING, in "Nature of the chemical bond", 3rd edn (Cornell University Press, Ithaca, New York, 1960) p. 644.
29. D. W. HYNDMAN, in "Petrology of igneous and metamorphic rocks" (McGraw-Hill, New York, 1972) p. 533.
30. A. C. LASAGA, in "Rate laws of chemical reactions", Reviews in Mineralogy Vol. 8 (BookCrafters, Chelsea, Minnesota, 1981) p. 398.
31. A. C. LASAGA, in "The atomistic basis of kinetics: defects in minerals", Reviews in Mineralogy Vol. 8 (BookCrafters, Chelsea, Minnesota, 1981) p. 398.

Received 10 May
and accepted 13 September 1993